Jurnal Ilmu Fisika
Vol. 17, No. 2, September 2025, pp. 125–134
ISSN: 1979-4657 (Print); 2614-7386 (Online)
https://doi.org/10.25077/jif.17.2.125-134.2025

Jurnal Ilmu Fisika
Open Access

A Kinetics Model of Amyloid-Beta (Aβ) in Alzheimer's Disease Using Euler and Fourth-order Runge-Kutta Methods

Cindyawati Cindyawati[1], Faozan Ahmad[2], Hendradi Hardhienata[2], Agus Kartono[2]

[1] Departement of Physics, Faculty of Sciences, Parahyangan Catholic University, Jalan Ciumbuleuit no. 94, Gedung 9, Bandung 40141, Indonesia
[2]Departement of Physics, Faculty of Mathematical and Natural Sciences, IPB University (Bogor Agricultural University), Jalan Meranti, Building Wing S, 2nd Floor, Kampus IPB Dramaga, Bogor 16680, Indonesia

Article Info

Article History:

Received February 16, 2025
Revised May 05, 2025
Accepted May 10, 2025
Published online May 13, 2025

Keywords:

Amyloid-beta (Aβ)
Alzheimer disease
Euler Method
Runge-Kutta Method
Mathematical model

Corresponding Author:

Cindyawati Cindyawati,
Email:
cindyawati_20200134@unpar.ac.id

ABSTRACT

Alzheimer's disease (AD) is a neurological disease that causes decreased brain function. It is known that the accumulation of amyloid-beta (Aβ) plaques in the brain is one of the causes of AD. The accumulation of Aβ plaques in the brain is a dynamic process; it begins with the growth of amyloid-beta monomers (M_1). Furthermore, amyloid-beta dimers (M_2) and so on, so that this collected into oligomers (O), fibrils (P), and plaques in the brain. This disrupts the communication pathways between nerve cells. In this study, each process of amyloid-beta plaque accumulation is presented with a mathematical model in the form of an ordinary differential equation. Therefore, the coupled ordinary differential equations are given for the entire process of Aβ plaque accumulation. In this study, this coupled model is calculated using numerical methods, such as the Euler and fourth-order Runge-Kutta methods. The Euler methods is simple and efficient, but its accuracy is low and can accumulate errors with larger step sizes. The fourth-order Runge-Kutta methods offers higher accuracy, better numerical stability, and greater control over the accuracy of the solution. These two numerical methods have never been compared for estimating numerical solutions of coupled ordinary differential equations.

1. INTRODUCTION

Alzheimer's disease (AD) is the most common cause of dementia, accounting for 60-80% of all dementia cases. Dementia is a general term for memory loss and other cognitive disorders that interfere with daily life. Alzheimer's disease is a specific type of dementia characterized by a progressive decline in brain cells. Dementia is not a single disease but rather a collection of symptoms associated with memory loss, difficulty thinking, reasoning, and other cognitive functions. Alzheimer's disease is also a neurodegenerative disease that causes brain cells to shrink and eventually die, affecting memory, language, and other cognitive abilities. Alzheimer's disease is the most common type of dementia because it is a progressive disease that affects the brain's ability to function properly over time (Li & Zhao, 2022). The main symptom of Alzheimer's patients is memory loss. Generally, elderly females aged over 65 years are more susceptible to this disease (Hao & Friedman, 2016). The death rate inflicted by Alzheimer's is very low. Based on data from the Statista Alzheimer's Association from 2000 to 2019, as many as 37 out of 100 thousand people, or around 0,037% died of Alzheimer's (Statista Alzheimer's Association, 2019). However, Alzheimer's patients in the world reached around 47 million people in

2016. This number is predicted to continue to grow until it reaches 131 million in 2050 (Asili et al., 2019). The care costs for Alzheimer's patients around the world are estimated at US$818 billion or the equivalent of 12 trillion rupiah (Prince et al., 2016). Therefore, Alzheimer's patients need to get special treatment because of the impact on social and economics.

The cause of AD is not yet known for certain, but the suspected cause of AD is the accumulation of amyloid-beta (Aβ) plaques. In Alzheimer's patients, Aβ plaques are found in the hippocampus. This study analyzed a kinetic model to describe how the evolutionary process of Aβ plaque accumulation causes biological changes in the brain and results in cognitive impairment, such as memory loss, difficulty performing simple tasks, and rapid emotional changes. Under normal conditions, the amyloid precursor protein (APP) is cleaved by α-secretase and γ-secretase. This process is called the non-amyloidogenic process and is soluble in the brain. As a result of the incorrect cutting of APP by β-secretase and γ-secretase, insoluble amyloid-beta monomers (M_1) are formed in the brain (Ackleh et al., 2021; Hampel et al., 2021). M_1 accumulated to form oligomers (O) and end up forming fibrils (P). This accumulation process is called the aggregation process. The fibril piles will settle and end up as plaque. This plaque disrupts the communication process between nerve cells (Ackleh et al., 2021).

Over the years, in the brains of Alzheimer's patients, there is a process of Aβ aggregation into plaques consisting of two stages, namely the nucleation and elongation stages (Naiki Hironobu, 1999; Ni et al., 2011). In Figure 1, the nucleation phase requires more energy, so it is thermodynamically less favorable. The process of forming Aβ monomers (M_1) into dimers (M_2), trimers (M_3), and oligomers (O) occurs more slowly. Meanwhile, the elongation phase requires less energy, which is a thermodynamically more favorable so that the transformation of oligomers (O) into fibrils (P) occurs in a short time.

The rate of concentration and growth of monomers into fibrils is described in the sigmoid graph in Figure 1 (Kumar & Walter, 2011).

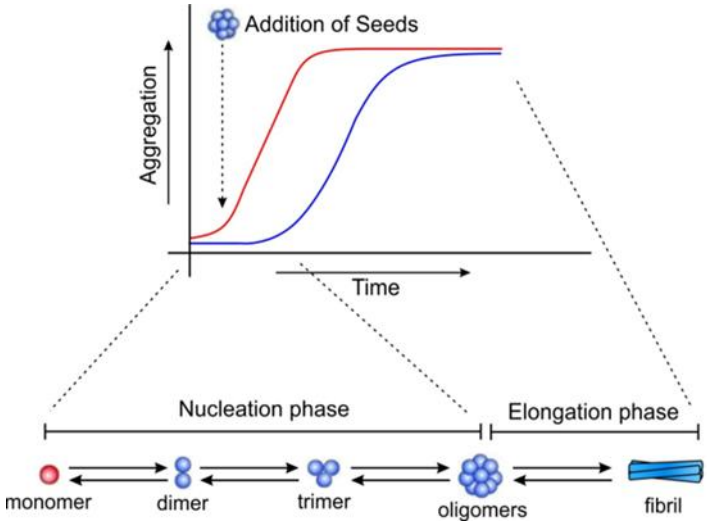

Figure 1. The process of growing amyloid-beta monomers (M_1) into fibrils (P) (Ackleh et al., 2021; Kumar & Walter, 2011)

Several studies have explored the growth kinetics of Aβ plaque from monomer to fibril, calculated based on its concentration rate, such as the works Ackleh co-workers (Ackleh et al. 2021). Therefore, the mathematical model chosen is the coupled ordinary differential equations. These coupled equations are in accordance with the description of the Aβ concentration buildup process. In this study, the Euler and fourth-order Runge-Kutta methods, which are commonly used numerical techniques to estimate the solution of ordinary differential equations, have been compared, especially for coupled ordinary differential equations.

The Euler methods is simple, efficient, and easy to implement computationally. This method is faster due to its simpler implementation and fewer function evaluations. However, it has lower accuracy and can accumulate errors with larger step sizes. Euler's method is a first-order numerical method that

approximates the solution of an ordinary differential equation by using the slope at a given point to estimate the solution at the next point in time. The basic formula for Euler's method is:

$$y(x+h) = y(x) + hf \tag{1}$$
$$y_{n+1} = y_n + hf(x_n, y_n) \text{ with } n = 0,1,2,3, \ldots$$

where $y(t)$ is the solution at time t, h is the step size (time), and $f(t, y(t))$ is the derivative of y concerning t. The fourth-order Runge-Kutta (RK4) method offers higher accuracy, better numerical stability, and more control over the solution's accuracy. This method has higher accuracy compared to the Euler method. However, it is a more complex implementation compared to the Euler method and requires more function evaluations per step. The RK4 method is generally more stable, meaning it is less prone to producing unstable solutions. The RK4 method is a more sophisticated numerical method that uses a weighted average of slopes at multiple points within a step to improve accuracy. The RK4 method involves calculating four different slopes (k_1, k_2, k_3, k_4) within each step and then using a weighted average of these slopes to update the solution. The RK4 method, which is used in general, can be written into the equations below:

$$k_1 = f(x_i, y_i) \tag{2}$$

$$k_2 = f\left(x_n + \frac{h}{2}, y_n + \frac{1}{2}k_1 h\right) \tag{3}$$

$$k_3 = f\left(x_n + \frac{h}{2}, y_n + \frac{1}{2}k_2 h\right) \tag{4}$$

$$k_4 = f(x_n + h, y_n + k_3 h) \tag{5}$$

$$y_{n+1} = y_n + \frac{h}{6}(k_1 + 2k_2 + 2k_3 + k_4) \tag{6}$$

with $n = 0,1,2,3, \ldots$

The Euler and RK4 methods can be derived from the Taylor series method. Both methods require careful selection of the step size (h) to balance accuracy and computational cost. The derivation of the Euler and RK4 methods from the Taylor series can be written into the equation below:

$$f(t+h) = \underbrace{\sum_{i=0}^{n} \frac{h^i}{i!} f^{(i)}(t)}_{\text{Approximation}} + \underbrace{\frac{h^{n+1}}{(n+1)!} f^{(n+1)}(\bar{t})}_{\text{Error}} \tag{7}$$

where $\bar{t}$ between t and $t+h$. In general, the RK4 method is chosen for solving ordinary differential equations, because it is more accurate and has a small error (Senthilnathan, 2018; Simangunsong & Mungkasi, 2021).

The Euler method is simple, while the RK4 method is complex and has a higher level of accuracy. The parameter used is the function evaluation per step. In the Euler method, the calculation is performed only once as shown in Equation (1), whereas in the RK4 method, the calculation is performed four times and then summed, as shown in Equations (2) to (6). Therefore, this study wants to analyze

the effect of the level of accuracy on the concentration rate of Aβ plaque growth by comparing the use of the two methods. Until now, there has been no research comparing the two methods, so it is hoped that this research can provide predictions of the growth rate of Aβ plaque concentration over time.

2. METHOD

2.1 Mathematical Model

In this study, we carried out simulation calculations of the growth rate of Aβ concentration up to $n = 6$, and a comparison of the use of the Euler and RK4 methods have been reviewed up to $n = 3$. If no significant difference occurs, the growth of Aβ from $n = 4$ up to fibrils uses the Euler method. The use of the Euler method shows that the kinetics of the concentration rate of Aβ growth in Alzheimer's patients is more efficient and also simplifies the calculation of Aβ concentration over time.

The use of the Euler method can provide an estimate of the development of Aβ concentration with a certain level of accuracy, but this accuracy is limited because the Euler method uses first-order, $n = 1$. Meanwhile, the RK4 method uses an accuracy of fourth-order, $n = 4$, and involves several more complicated iterations, thus providing a numerical solution that is closer to the real solution. The mathematical model used refers to Ackleh et al. (2021) using $n = 6$, which can be written into the equations:

$$\begin{aligned}
\frac{dM_1(t)}{dt} &= \delta M_1(t)\left(1-\frac{M_1(t)}{\gamma}\right) - 2K_1M_1^2(t) - M_1(t)\sum_{i=2}^{n-1} K_iM_i(t), \\
&-(O_a-n)K_6M_1(t)M_6(t) - (P_a-O_a)K_OM_1(t)O(t) - \mu_1M_1(t), \\
\frac{dM_2(t)}{dt} &= K_1M_1^2(t) - K_2M_1(t)M_2(t) - \mu_2M_2(t), \\
&\vdots \\
\frac{dM_6(t)}{dt} &= K_5M_1(t)M_5(t) - K_6M_1(t)M_6(t) - \mu_6M_6(t), \\
\frac{dO(t)}{dt} &= K_6M_1(t)M_6(t) - K_OM_1(t)O(t) - \mu_OO(t), \\
\frac{dP(t)}{dt} &= K_OM_1(t)O(t) - \mu_pP(t)
\end{aligned} \tag{8}$$

Equations 8 shows the coupled ordinary differential equations for the formation of monomers (M_1) into fibrils (P). O_a and P_a are the average sizes of oligomers and fibrils. Assumed that the production of monomer (M_1) is represented by the saturation function $f(M_1)M_1 = \delta M_1\left(1-\frac{M_1}{\gamma}\right)$ where δ indicates the average growth of the monomer and γ indicates the transport capacity. This function was chosen considering that the monomer concentration will continue to grow. Second, there is a process of cleaning up the Aβ heap which is denoted as μ_i. The factors $(O_a - n)$ and $(P_a - O_a)$ in Equations (9) indicate the average amount of monomers that need to be added to the M_n aggregates to form oligomers and the average amount of monomers that need to be added to oligomers to form fibrils. The parameters used in this mathematical equation are listed in Table 1

2.2 Numerical Method

Numerical equations were calculated using the Euler and RK4 methods with a period of 100 days and step size ($h = \Delta t$) is 0,01 day. This study uses a very small step size ($h = \Delta t$) for both methods, which aims to provide the same level of accuracy. It also shows that when the value of $h = \Delta t$ is the smallest, the Euler method curve approaches the RK4 method. Both of these methods have

been run by MATLAB R2021a software. Equations (8) was written into a script in MATLAB. The Euler and RK4 methods were applied manually. Initial conditions and parameters refer to Ackleh et al (2021). The following are the initial conditions and parameters used:

$$\delta = 50, \gamma = 75, K_1 = 10^{-4}, K_2 = 5 \times 10^{-4}, K_3 = 10^{-3}, K_4 = 5 \times 10^{-3}, K_5 = 10^{-2}, K_6 = 5 \times 10^{-2}, K_O = 0{,}1, n = 6, O_a = 10, P_a = 100, \mu_1 = \mu_2 = \mu_3 = \mu_4 = \mu_5 = \mu_6 = 10^{-3}, \mu_O = 10^{-4}, \mu_P = 10^{-5} \quad (9)$$

$$M_1 = 10, M_2 = M_3 = M_4 = M_5 = M_6 = O = P = 0 \quad (10)$$

All initial conditions are expressed in units of gr/ml.

Table 1. Parameters, descriptions, and estimates based on reference to the Alzheimer's model

Parameter	Meaning	Estimate	Reference
$K_1 - K_6$	Nucleation rate	$10^{-6} - 10^{-4} M^{-1} s^{-1}$	(Cohen et al., 2012; Knowles et al., 2009)
K_O	Elongation rate	$10^{-1} - 10^{4} M^{-1} s^{-1}$	(Cohen et al., 2012; Craft et al., 2002; Knowles et al., 2009; Lomakin et al., 1997)
O_a	Average oligomer size	$2 - 10$	(Fraser et al., 1991; Hill et al., 2009; Linse, 2017)
P_a	Average fibril size	$10 - 10^{3}$	(Lomakin et al., 1997)
$\mu_1 - \mu_6$	Degradation rate of monomers	$10^{-5} - 10^{-3} s^{-1}$	(Craft et al., 2002; Hao & Friedman, 2016)
μ_O	Degradation rate of oligomers	$10^{-6} - 10^{-4} s^{-1}$	(Hao & Friedman, 2016)
μ_P	Degradation rate of fibrils	$10^{-7} - 10^{-5} s^{-1}$	Estimated

3. RESULTS AND DISCUSSION

After performing calculations with both method, graphs of the growth of the amyloid-beta monomer (M_1) into fibrils (P) are obtained along with its concentration rate. Figure 2 shows a graph that has a sigmoid curve output. The sigmoid curve is the initial input for the amyloid-beta (Aβ) accumulation process.

The nucleation stage starts from the formation of monomers (M_1) to the formation of amyloid-beta oligomers (O) (Figure 1). This is shown on the M_1, M_2, M_3, and O graphs in Figures 3(a)-(d) which will then experience saturation at a certain time. After the oligomer is formed, it enters the elongation stage where the oligomer became a fibril. This is shown in the P graph in Figure 3(e).

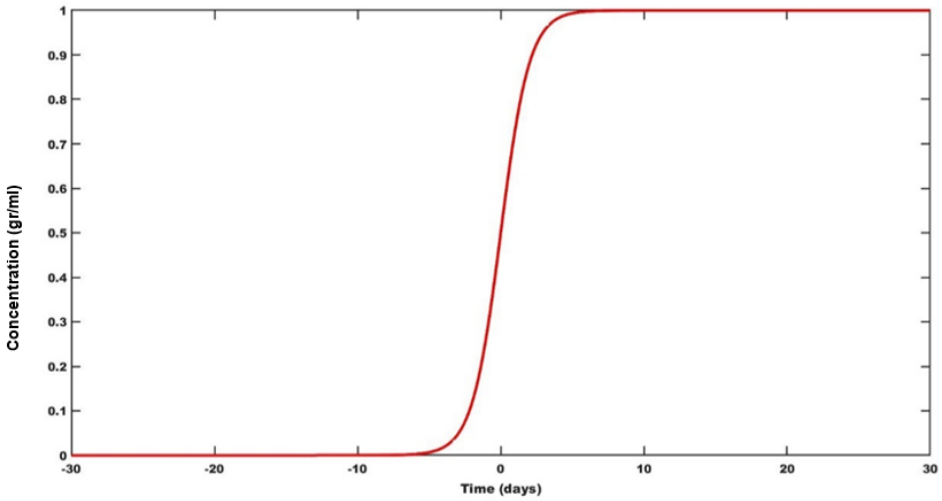

Figure 2. Sigmoid curve as the main input.

In Figure 3(a)–(e), the red and blue lines represent the simulation results obtained using the Euler and RK4 methods, respectively. These results describe the progression of amyloid-beta aggregation over a 100-day period. The process initiates with the monomeric form (M_1), which gradually aggregates into dimers (M_2). M_1 and M_2 further interact to form trimers (M_3), which subsequently assemble into oligomers (O). As aggregation continues, oligomers form fibrils (P), and eventually, these fibrils accumulate into plaques in the brain.

Throughout the simulation, the concentration of M_1 shows a slight and consistent decline, reflecting its role as a precursor consumed during aggregation. M_2 increases rapidly in the initial phase, indicating fast dimer formation, but then levels off as M_2 is further used in M_3 formation. For M_3 and O, the concentration grows during the first 10 days, continues increasing steadily until day 40, and then plateaus, suggesting a saturation in intermediate species production. Meanwhile, P exhibits a continuous increase until day 40, after which its concentration remains stable, indicating the completion of fibrillization.

These trends reflect the sequential and time-dependent nature of amyloid-beta aggregation and are consistent with biological observations, where early oligomer formation precedes plaque development associated with neurodegenerative progression.

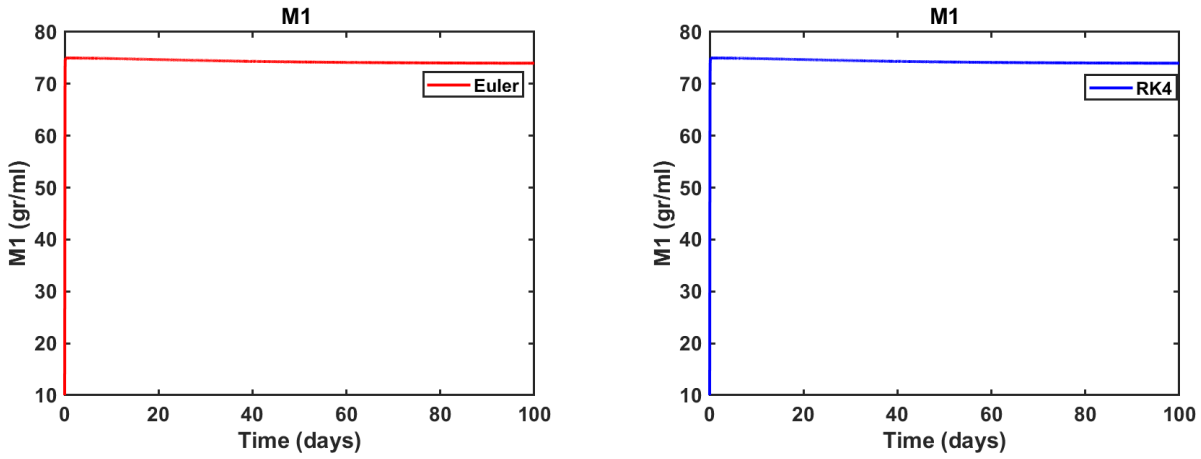

Figure 3(a). Amyloid-beta monomers aggregation process in 100 days.

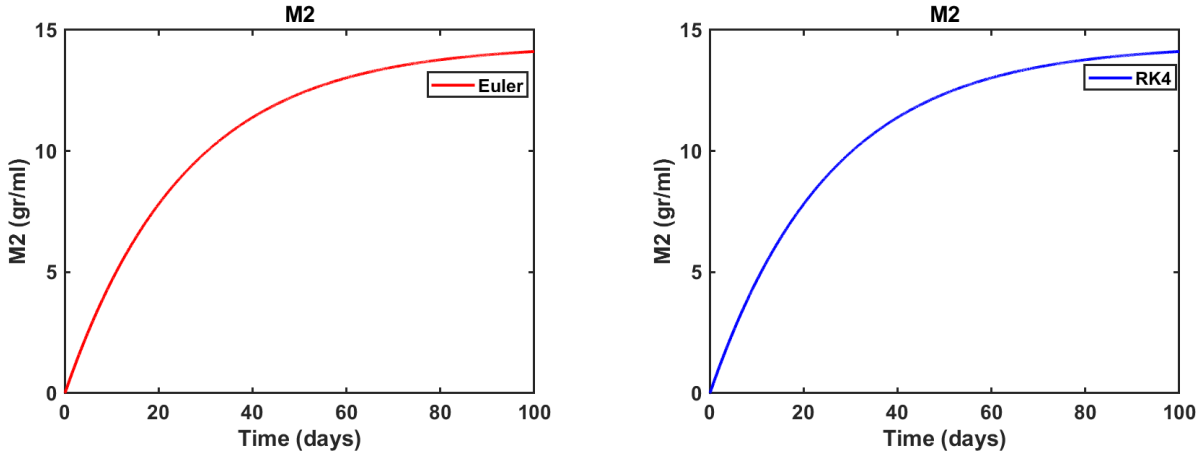

Figure 3(b). Amyloid-beta dimers aggregation process in 100 days.

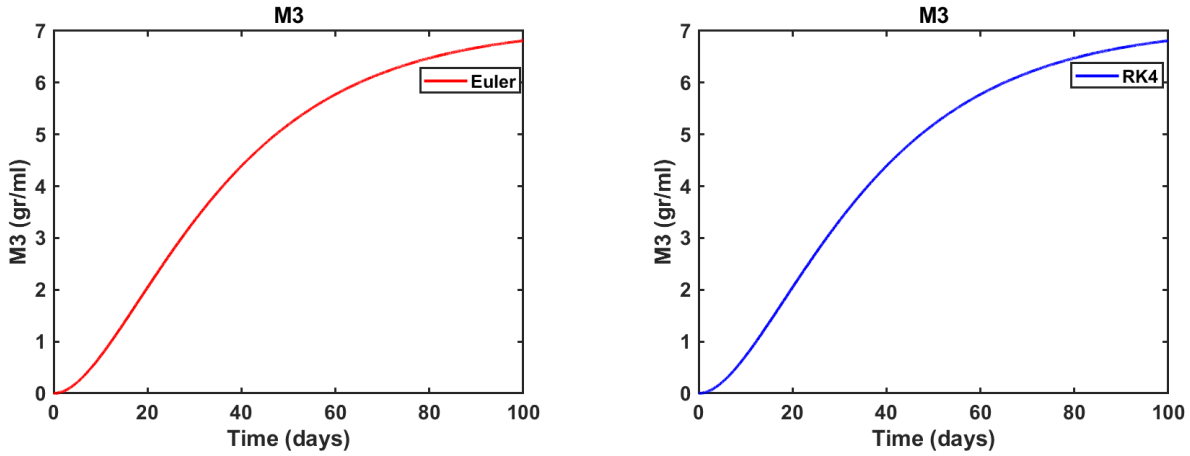

Figure 3(c). Amyloid-beta trimer aggregation process in 100 days.

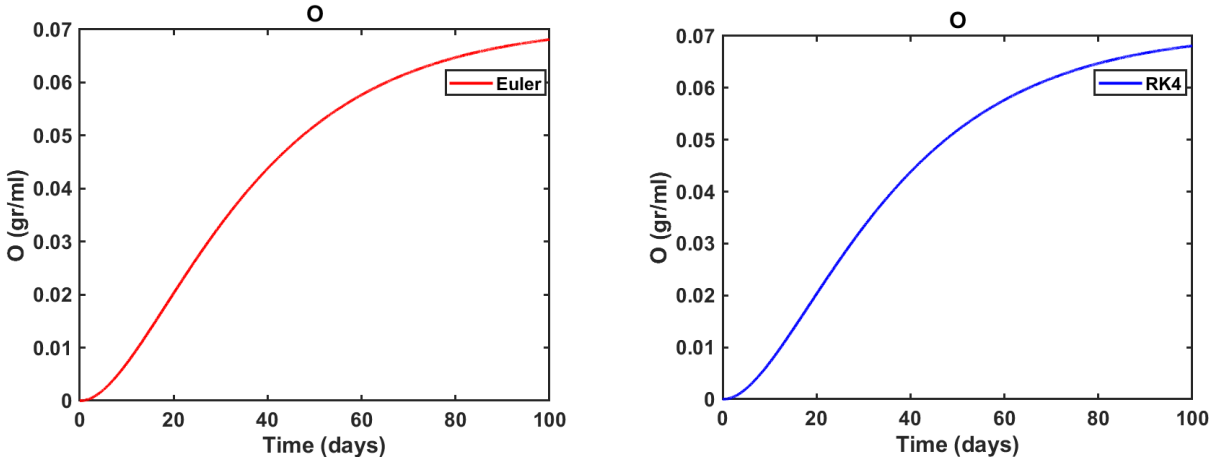

Figure 3(d). Amyloid-beta oligomers aggregation process in 100 days.

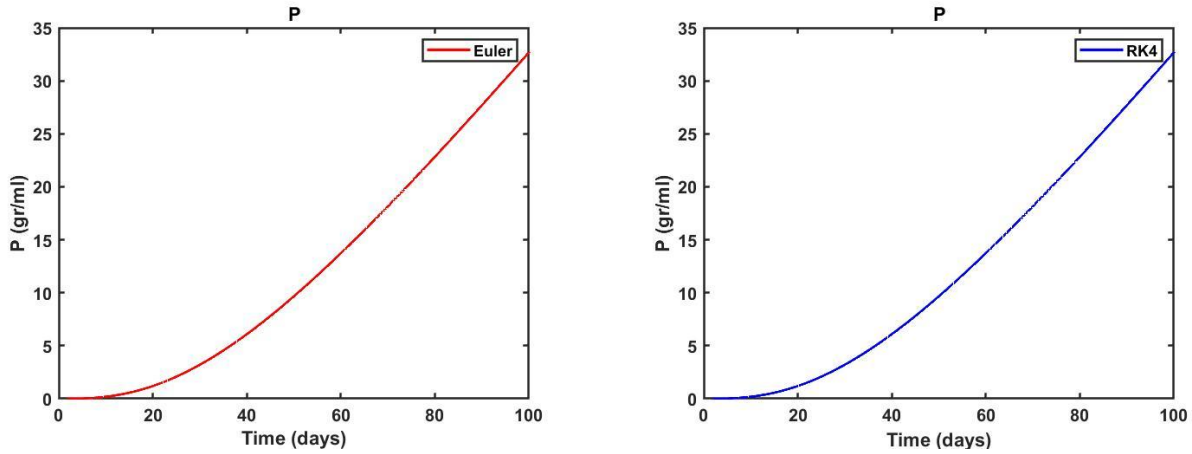

Figure 3(e). Amyloid-beta fibrils aggregation process in 100 days.

Based on the results of the calculation simulation at n = 3 shown in Figure 3(c), it appears that there is no significant difference in predicting the growth rate of amyloid-beta (Aβ) using either the Euler or the RK4 methods. The level of accuracy in this simulation has no effect, because the selection of step size ($h = \Delta t$) is very small for both methods. Therefore, n = 4 up to n = 6 are simply calculated by using the Euler method. Figure 4 shows the calculation results of the amyloid-beta (Aβ) aggregation process at n = 4 up to n = 6 on 100 days.

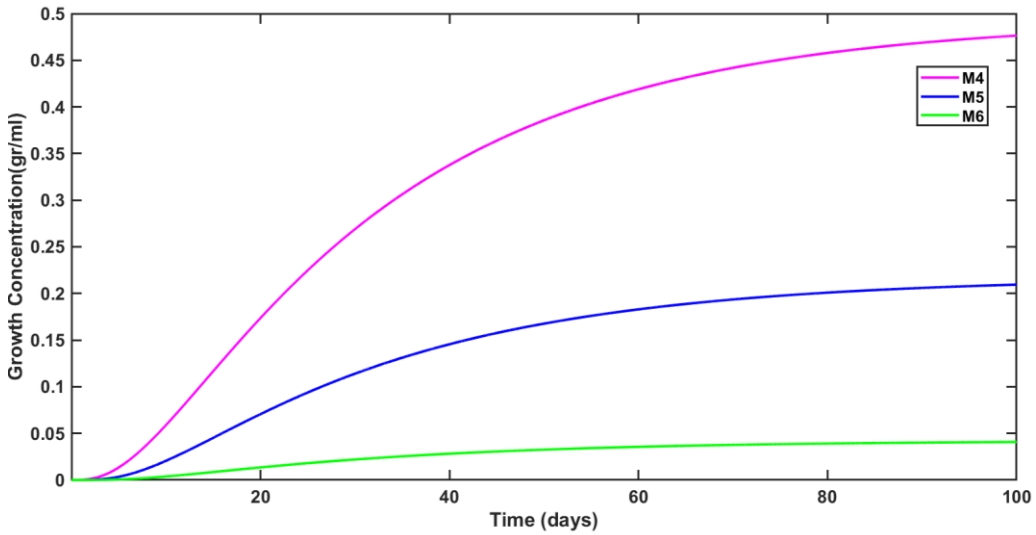

Figure 4. Amyloid-beta (Aβ) aggregation process in 100 days for M4 up to oligomer (O) using Euler method.

Based on Figure 4, M_4 graph shows that the amyloid-beta (Aβ) concentration rate increased from the start to 10th day. Then on the 10th to the 40th day, it continued to grow at a constant rate, and on the 40th to the 100th day it slows down the growth. The same thing also happened on the M_5 and M_6 graphs. Thus, the addition of amyloid-beta monomer to the simulation did not have any significant effect because based on biogically this is caused by amyloid-beta has started to form fibrils.

Based on the simulation results of this study, the difference in the rate of amyloid-beta concentration occurred significantly in M_2. The differences in the structure of monomers to oligomers of amyloid-beta affect the rate of growth concentration (Lindstrom et al., 2021). The choice of parameters and initial values may influence the simulation results.

4. CONCLUSION

The kinetics of Alzheimer's disease based on the growth rate of amyloid-beta (Aβ) plaque concentration is simulated using coupled ordinary differential equations. Based on the simulation results in this study, it is concluded that there is no difference in the simulation results between the Euler method and the RK4 method in predicting amyloid-beta concentration in Alzheimer's patients. The level of accuracy in both methods does not affect the prediction of amyloid-beta (Aβ) plaque growth concentration, with the selection of a step size value ($h = \Delta t$) of 0,01 day. This study suggests choosing a simple and computationally efficient method to be used in coupled ordinary differential equation problems, with the condition of selecting a small step size value ($h = \Delta t$).

REFERENCE

Ackleh, A. S., Elaydi, S., Livadiotis, G., & Veprauskas, A. (2021). A continuous-time mathematical model and discrete approximations for the aggregation of β-Amyloid. *Journal of Biological Dynamics*, 15(1), 109–136. https://doi.org/10.1080/17513758.2020.1869843

Asili, E., Yarahmadian, S., Khani, H., & Sharify, M. (2019). A Mathematical Model for Amyloid- β Aggregation in the Presence of Metal Ions: A Timescale Analysis for the Progress of Alzheimer Disease. *Bulletin of Mathematical Biology*. https://doi.org/10.1007/s11538-019-00583-3

C.Senthilnathan. (2018). A Numerical Solutions Of Initial Value Problems (Ivp) For Ordinary Differential Equations (Ode) With Euler And Higher Order Of Runge Kutta Method Using Matlab. *International Journal of Engineering Science Invention (IJESI)*, 7(4), 25–31.

Cohen, S. I. A., Vendruscolo, M., Dobson, C. M., & Knowles, T. P. J. (2012). From macroscopic measurements to microscopic mechanisms of protein aggregation. *Journal of Molecular Biology*, 421(2–3), 160–171. https://doi.org/10.1016/j.jmb.2012.02.031

Craft, D. L., Wein, L. M., & Selkoe, D. J. (2002). A mathematical model of the impact of novel treatments on the Aβ burden in the Alzheimer's brain, CSF and plasma. *Bulletin of Mathematical Biology*, 64(5), 1011–1031. https://doi.org/10.1006/bulm.2002.0304

Fraser, P. E., Duffy, L. K., O'Malley, M. B., Nguyen, J., Inouye, H., & Kirschner, D. A. (1991). Morphology and antibody recognition of synthetic β-amyloid peptides. *Journal of Neuroscience Research*, 28(4), 474–485. https://doi.org/10.1002/jnr.490280404

Hampel, H., Hardy, J., Blennow, K., Chen, C., Perry, G., Kim, S. H., Villemagne, V. L., Aisen, P., Vendruscolo, M., Iwatsubo, T., Masters, C. L., Cho, M., Lannfelt, L., Cummings, J. L., & Vergallo, A. (2021). The Amyloid-β Pathway in Alzheimer's Disease. *Molecular Psychiatry*, 26(10), 5481–5503. https://doi.org/10.1038/s41380-021-01249-0

Hao, W., & Friedman, A. (2016). Mathematical model on Alzheimer's disease. *BMC Systems Biology*, 10(1), 1–18. https://doi.org/10.1186/s12918-016-0348-2

Hill, S. E., Robinson, J., Matthews, G., & Muschol, M. (2009). Amyloid protofibrils of lysozyme nucleate and grow via oligomer fusion. *Biophysical Journal*, 96(9), 3781–3790. https://doi.org/10.1016/j.bpj.2009.01.044

Knowles, T. P. J., Waudby, C. A., Devlin, G. L., Cohen, S. I. A., Aguzzi, A., Vendruscolo, M., Terentjev, E. M., Welland, M. E., & Dobson, C. M. (2009). An analytical solution to the kinetics of breakable filament assembly. *Science*, 326(5959), 1533–1537. https://doi.org/10.1126/science.1178250

Kumar, S., & Walter, J. (2011). Phosphorylation of amyloid beta peptides. *Aging*, 3(8), 803–812. https://doi.org/10.18632/aging.100362

Lede, Y. K., & Mungkasi, S. (2019). Performance of the Runge-Kutta method in solving a mathematical model for the spread of dengue fever disease. *AIP Conference Proceedings*, 2202. https://doi.org/10.1063/1.5141657

Li, H., & Zhao, H. (2022). Mathematical model of Alzheimer's disease with prion proteins interactions and treatment. *Applied Mathematics and Computation*, 433, 127377. https://doi.org/10.1016/j.amc.2022.127377

Lindstrom, M. R., Chavez, M. B., Gross-Sable, E. A., Hayden, E. Y., & Teplow, D. B. (2021). From reaction kinetics to dementia: A simple dimer model of Alzheimer s disease etiology. *PLoS Computational Biology*, 17(7), 1–24. https://doi.org/10.1371/journal.pcbi.1009114

Linse, S. (2017). Monomer-dependent secondary nucleation in amyloid formation. *Biophysical Reviews*, 9(4), 329–338. https://doi.org/10.1007/s12551-017-0289-z

Lomakin, A., Teplow, D. B., Kirschner, D. A., & Benedeki, G. B. (1997). Kinetic theory of fibrillogenesis of amyloid β-protein. *Proceedings of the National Academy of Sciences of the United States of America*, 94(15), 7942–7947. https://doi.org/10.1073/pnas.94.15.7942

Naiki Hironobu, G. F. (1999). Kinetic analysis of amyloid fibril formation. Method in Molecular Biology, 309, 305–318. https://doi.org/10.1007/978-1-4939-7816-8_12

Ni, C., Shi, H., Yu, H., Chang, Y., & Chen, and Y. (2011). Folding stability of amyloid-β 40 monomer is an important determinant of the nucleation kinetics in fibrillization. *The FASEB Journal*, 25(4), 1390–1401. https://doi.org/10.1096/fj.10-175539

Prince, M., Comas-Herrera, A., Knapp, M., Guerchet, M., & Karagiannidou, M. (2016). World Alzheimer Report 2016 Improving healthcare for people living with dementia. Coverage, Quality and costs now and in the future. *Alzheimer's Disease International* (ADI).

Simangunsong, L., & Mungkasi, S. (2021). Fourth order Runge-Kutta method for solving a mathematical model of the spread of HIV-AIDS. AIP Conference Proceedings, 2353. https://doi.org/10.1063/5.0052550

Statista Alzheimer's Association. (2019). statistic_id452945_death-rate-due-to-alzheimers-disease-in-the-us-2000-2019.pdf.